JOURNAL OF AIRCRAFT
Vol. 31, No. 1, Jan.–Feb. 1994

Integrated Structure/Control Concepts for Oblique Wing Roll Control and Trim

Terrence A. Weisshaar*
Purdue University, West Lafayette, Indiana 47907

The integrated design problem posed by the need for oblique wing aircraft aeroelastic roll trim at subsonic airspeeds is examined. It is shown that the need for roll trim is reduced when structural tailoring with advanced composite materials is used, but there is a maximum oblique wing sweep angle above which tailoring is ineffective. A formula for this sweep angle is developed. The need for a combination of asymmetrical aileron input and aeroelastic tailoring of a laminated wing structure is also examined. The design tradeoff between structural tailoring, to reduce the need for ailerons for roll trim, and aileron control surface effectiveness to provide roll trim is illustrated using an example configuration. Tailoring the aileron size so that the aileron reversal dynamic pressure and the static aeroelastic divergence dynamic pressure of the restrained oblique wing are identical is also discussed.

Introduction

Oblique Wing Static Aeroelasticity

TWO features of an oblique wing aircraft, such as that sketched in Fig. 1, appear to make it well-suited to transport aircraft use as well as combat aircraft.[1,2] The ability to sweep the wing in flight allows the plane to takeoff with the wing unswept, permitting a shorter takeoff distance and more rapid climbout when compared to a similar, symmetrical swept wing aircraft. Vaiable sweep allows the wing to move as a unit to reduce drag as speed increases. The low wave drag of the oblique wing at supersonic speeds makes it a candidate for an interceptor fighter or a long-range strike aircraft with good loiter capability when the wing is unswept.

Oblique wing asymmetry creates several unusual design problems. Among these are 1) pitch-yaw-roll aerodynamic coupling, 2) spanwise boundary-layer flow, and 3) asymmetrical wing aeroelastic behavior. Because forward swept and aft swept wings have drastically different static aeroelastic features, lift asymmetry may be significant in some speed regimes.[3] The purpose of this article is to investigate the control of spanwise lift asymmetry created both by oblique wing geometric asymmetry and unsymmetrical bending deformation, and to point out design tradeoffs that may arise. This control may arise from the design of the wing structure, the design of the aileron surfaces, or a combination of both. The design of an aeroelastically tailored laminated wing structure must be able to minimize spanwise lift asymmetry, but, at the same time, preserve enough aileron rolling moment effectiveness so that the aircraft can be trimmed effectively in roll.

Figure 2 illustrates the basic problem to be addressed. It shows two subsonic, spanwise lift distributions present on an initially untwisted 30-deg oblique wing (clamped to a fixed support at the wing root) operating subsonically at 75% of its divergence speed. In both cases, the streamwise angle of attack at the root is the same. In one case the wing structure is assumed to be rigid; the second case includes the aeroelastic effects of wing bending and torsional flexibility. The curve labeled "rigid wing" illustrates the basic lift asymmetry created by spanwise inflow from the tip of the swept forward wing portion towards the aft swept tip. This lift unbalance creates an unbalanced rolling moment that is resisted by the support. The curve labeled "flexible wing" has exactly the opposite tendency, since wing bending deflection creates further spanwise lift distortion.

The reasons for this deformation-induced distortion are clear when one examines Fig. 3. From the streamwise perspective shown in Fig. 3a, bending of a conventional swept back wing produces a reduced angle of attack or washout. On the other hand, bending of the forward swept portion of the wing produces wash-in, an increased streamwise angle of attack, seen when Fig. 3a is viewed with the airflow coming from the right. The amount of lift distortion depends upon wing aeroelastic flexibility, involving a combination of flight speed, altitude, and wing structural stiffness.

Forward sweep promotes "destiffening" of the wing and a buildup of lift for a fixed angle of attack at the root. At a critical combination of dynamic pressure, bending stiffness, and planform shape, the aerodynamic forces created by forward swept wing distortion will balance the structural restoring forces created by the wing distortion. This critical dynamic pressure is called the divergence dynamic pressure. At higher airspeeds, unopposed wing distortion or "aeroelastic divergence" takes place until wing structural failure or some other equally undesirable event occurs.

It should be mentioned that, while aeroelastic divergence is the primary mode of instability of a restrained oblique wing,

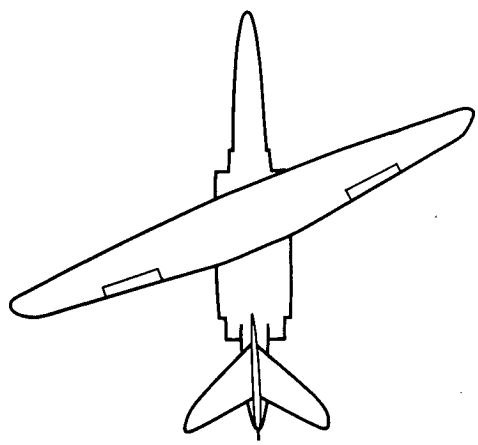

Fig. 1 Hypothetical oblique wing aircraft configuration.

Received Sept. 20, 1992; revision received Oct. 30, 1992; accepted for publication Nov. 3, 1992.

*Professor, School of Aeronautics and Astronautics, 1282 Grissom Hall. Fellow AIAA.

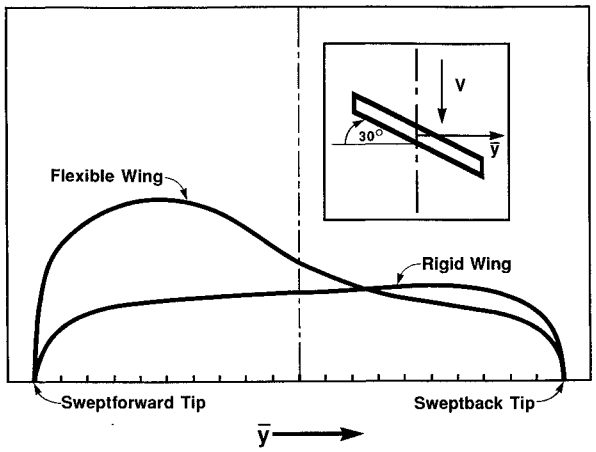

Fig. 2 Oblique wing spanwise lift distributions: 30-deg swept, uniform planform wing operating at 75% of its divergence speed, with the wing root clamped at its centerline, excluding and including wing flexibility.

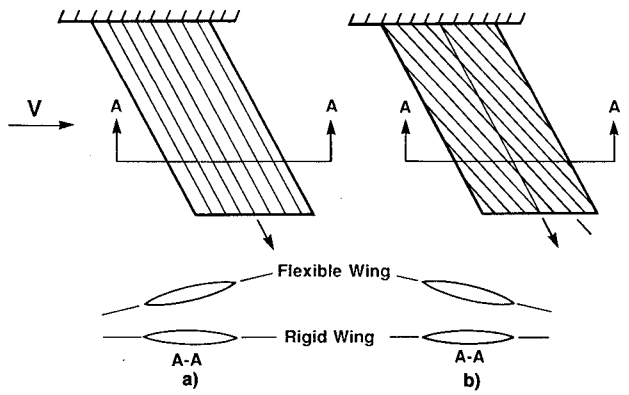

Fig. 3 Streamwise angle of attack induced by swept back wing bending: a) orthotropic wing without tailoring (washout) and b) with ply reorientation (wash-in).

an oblique wing in flight is free to roll, pitch, and plunge in response to an external disturbance. As a result, a coupled wing/body, "body-freedom" flutter, not wing divergence, is the most likely mode of oblique wing aeroelastic instability.[4–6] However, the clamped wing divergence speed remains an important bench mark because its value defines the dynamic pressure near which static aeroelastic flexibility effects are likely to be significant.

To reduce spanwise lift asymmetry of the type illustrated in Fig. 2, the local streamwise angles of attack can be altered by building the wing with a distorted form or "jig twist," tailored for a specific flight condition. As an alternative, asymmetrical aileron deployment can decrease outboard lift on one wing and increase it on the other. This requires a flight control system that allows differential aileron rotation—when one aileron is deflected downward, the other is deflected upward. The effectiveness of both jig twist and ailerons for roll control of oblique wings constructed of metallic materials is discussed in Ref. 7.

Aeroelastic lift distortion of the type illustrated in Fig. 2b could be eliminated by designing a very stiff wing, but this would lead to a weight penalty. An alternate approach to stiffening the wing is to accept bending distortion, but to couple it together with another favorable type of deformation. This is the approach adopted by aeroelastic tailoring,[8,9] and one purpose of this article is to examine the use of laminate directional stiffness (such as is illustrated in Fig. 3b) to control unfavorable static aeroelastic dissimilarities between the forward swept wing and aft swept wing portions of an oblique wing aircraft. Aeroelastic stiffening of the forward swept wing and aeroelastic destiffening of the aft swept wing through manipulation of the amount of bend/twist stiffness cross coupling (by ply orientation) can reduce the oblique wing roll tendency. The interaction between aerodynamic loads and structural flexibility creates the problem, but also provides the necessary authority to overcome the problem.

In some situations ailerons still may be desirable for roll trim. Proper laminate design can also enhance aileron roll effectiveness. Fung[10] discusses the relationships between divergence speed, aileron effectiveness, and reversal of a two-dimensional airfoil section. He indicates that the most effective aileron size occurs when aileron reversal and divergence dynamic pressures are equal (Ref. 10, p. 118).

With a three-dimensional wing of the type we are considering, both aileron effectiveness and divergence speed depend upon wing stiffness and geometry. However, the aileron effectiveness also depends upon the spanwise position and size of the aileron. Simultaneous matching of control surface parameters, such as size and position to aeroelastic requirements, has not been given extensive attention. However, the few references that are available indicate that this type of activity may be profitable.[11,12]

This article will examine the tradeoffs between passive control of an aeroelastically induced roll moment through laminate reorientation and the aileron's ability to provide roll trim. A nondimensional laminate stiffness cross coupling parameter will be defined and used for the study. Illustrative results developed using a simple configuration will be used to identify a design optimization opportunity. We will begin with a discussion of an analytical model that will be used to describe wing aeroelastic behavior.

Analytical Model

To capture the essential features of oblique wing aeroelastic phenomena and to study parametric tradeoffs, previously cited studies used simplistic aeroelastic models with reasonable confidence. For roll trim studies, however, more sophisticated aerodynamic models are advisable. The computational scheme used for the present study is based upon that outlined in NACA TN 3030[13] and also parallels closely techniques discussed in Ref. 14. It is restricted to subsonic Mach numbers, but combines accuracy and economy in a measure necessary to achieve reliable, but computationally inexpensive results.

The wing is assumed to be of moderate-to-high-aspect ratio and to behave as a flexible beam-like structure. Modifications of Ref. 13 to account for beam-like laminate bend/twist cross coupling (of the type shown in Fig. 3b), are developed in Ref. 15. The aerodynamic representation is shown in Fig. 4.

This figure shows a wing planform subdivided into a discrete number of spanwise panels. The spanwise lift distribution is modeled as a system of horseshoe vortices, each of constant strength Γ_j. The strength of these vortices is related to the magnitude of the lift per unit length p_j on each panel. With this idealization, the left and right wing portions are aero-

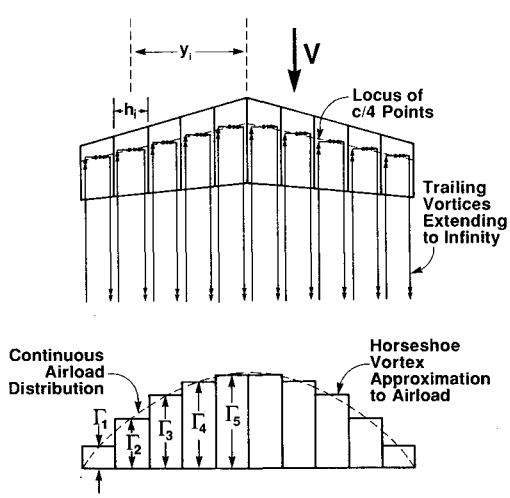

Fig. 4 Wing spanwise lift idealization showing horseshoe vortices with strength Γ_i attached at panel ¼-chord locations.

dynamically interactive. The lift intensity at the finite number of panels along the wing is represented as a column vector $\{p_j\}$, while the streamwise angle-of-attack distribution at the same positions is $\{\alpha_i\}$. A linear relationship between $\{p_j\}$ and $\{\alpha_i\}$ is written as follows:

$$1/q[A_{ij}]\{p_j\} = \{\alpha_i\} \tag{1}$$

The square matrix $[A_{ij}]$ is composed of aerodynamic influence coefficients; q denotes the dynamic pressure. This matrix depends upon planform geometry (spanwise and chordwise dimensions and wing sweep) and the two-dimensional lift curve slope c_{l_α} of each panel cross section. The elements A_{ij} are Mach number dependent; this computational procedure is restricted to subsonic Mach numbers. If the vector $\{\alpha_i\}$ is known, the relationship in Eq. (1) may be inverted to solve for $\{p_j\}$.

With aeroelastic interaction, the angle-of-attack distribution $\{\alpha_i\}$ is the result of three distinct vector components, expressed as follows:

$$\{\alpha_i\} = \{\alpha_r\} + \{\alpha_s\} + \{\alpha_c\} \tag{2}$$

In Eq. (2), the vector $\{\alpha_r\}$ represents an array (note that dummy indices are omitted for clarity) of panel "rigid body" streamwise angles of attack present at zero airspeed. This vector is due to a combination of the wing pitch angle and "built-in" geometric angle of attack distribution (due to jig twist or gravity induced "droop") along the wing. The vector $\{\alpha_s\}$ represents the streamwise angle-of-attack distribution caused by wing structural bending and twisting deformation. The elements of this vector are functions of wing flexibility and airspeed, but are initially unknown. The $\{\alpha_c\}$ distribution represents the spanwise angle-of-attack distribution created by aileron deflection.

The panel angles of attack due to structural deformation under load are determined from the following equation:

$$\{\alpha_s\} = [C_{ij}]\{p_j\} \tag{3}$$

where C_{ij} represents an element of the wing structural flexibility matrix. The computation of this matrix requires that each oblique wing semispan be fully restrained (clamped) at its root. The structural influence coefficients C_{ij} depend upon wing cross-sectional bending stiffness EI, torsional stiffness GJ, and a bend/twist stiffness cross coupling parameter K.[15] This latter parameter is controlled by laminate design, specifically ply orientation, and may be positive, negative, or zero. A bounded, nondimensional measure of bend/twist deformation coupling is defined as

$$\Psi^2 = K^2/(EI \cdot GJ) \qquad (\Psi^2 < 1) \tag{4}$$

The stiffness parameters EI, GJ, and K are measured with respect to a swept spanwise reference axis. The usual location of this reference axis is the locus of shear centers when $K = 0$. As a result, the matrix $[C_{ij}]$ depends upon the wing sweep angle. The details of the formulation of this matrix are discussed in Ref. 15.

Equations (1–3) provide a relationship between aeroelastic spanwise lift and the initial spanwise panel angles of attack. This relationship reads as follows:

$$[B_{ij}]\{p_j\} = \{\alpha_r\} + \{\alpha_c\} \tag{5}$$

where

$$[B_{ij}] = (1/q[A_{ij}] - [C_{ij}]) \tag{6}$$

The negative of $[B_{ij}]$ is the aeroelastic flexibility matrix; it is a function of Mach number and the flight dynamic pressure q. Note that the solution for $\{p_j\}$ requires the inverse of $[B_{ij}]$; this matrix may be singular at certain "critical" values of q. These values are eigenvalues of $[B_{ij}]$. The lowest nonnegative, real value of q, denoted as q_D, that makes the determinant of $[B_{ij}]$ equal to zero corresponds to the clamped wing static divergence dynamic pressure. For some symmetrical wings, particularly those with moderate sweepback, real values of q do not exist, so divergence will not occur.

The deflection of a control surface causes a change in apparent local angle of attack, created by a control induced airfoil camber change that rotates the position of the zero lift line of the panel to which the control surface is attached. This change is written as the ratio of two aerodynamic sectional coefficients

$$\alpha_c = \frac{\partial \alpha}{\partial \delta}\,\delta_0 = \left(\frac{c_{l_\delta}}{c_{l_\alpha}}\right)\delta_0 \tag{7}$$

where δ_0 is the control surface rotation angle. Control deflection also creates a distributed spanwise twisting moment that twists the wing. Adding these two effects together, the twist $\{\alpha_c\}$ is written as follows:

$$\{\alpha_c\} = \{\gamma_i\}\frac{\partial \alpha}{\partial \delta}\,\delta_0 + q[E_{ij}]\{\gamma_j\}c_{m\delta}\delta_0 \tag{8}$$

The elements E_{ij} are functions of wing planform geometry, wing sweep, stiffness cross coupling, and cross-sectional bending stiffness, and torsional stiffness.[15] The choice of the elements of the vector $\{\gamma_i\}$ locates the spanwise position of aileron elements. A wing panel without an aileron segment has $\gamma_i = 0$. A panel with the aileron deflected downward an amount δ_0, has $\gamma_i = +1$, while an upward aileron rotation is represented by $\gamma_i = -1$. Equation (8) is written with the assumption that control surface sectional characteristics ($c_{m\delta}$ and $\partial\alpha/\partial\delta$) are identical for all aileron panels, although differences can be accounted for using this approach.

Combining the previous equations, the spanwise lift distribution vector is computed using the following equation:

$$\{p_i\} = [B_{ij}]^{-1}\{\alpha_r\} + q[B_{ij}]^{-1}[E_{ij}]\{\gamma_j\}c_{m\delta}\delta_0 + [B_{ij}]^{-1}\{\gamma_j\}\frac{\partial \alpha}{\partial \delta}\,\delta_0 \tag{9}$$

Aircraft roll equilibrium requires that the roll moment about the wing centerline due to $\{p_i\}$ be zero, and that the total lift be equal to the weight of the aircraft. In terms of panel width h_i (shown in Fig. 4), and the distance of each panel midspan from the roll axis y_i (also shown in Fig. 4), the roll equilibrium condition is written as

$$\{y_i\}^T\{p_i h_i\} = 0 \tag{10}$$

The asymmetrical aileron deflection required for oblique wing roll equilibrium (roll "trim") may be found by combining Eqs. (9) and (10):

$$\delta_0 = \frac{-\{y_i h_i\}^T[B_{ij}]^{-1}\{\alpha_r\}}{\{y_i h_i\}^T[B_{ij}]^{-1}\left[\{\gamma_j\}\dfrac{\partial \alpha}{\partial \delta} + q[E_{ij}]\{\gamma_j\}c_{m\delta}\right]} \tag{11}$$

However, unless the wing is operating in a wind tunnel at a fixed angle of attack, the aircraft "lift trim" condition determines the wing angle of attack $\{\alpha_r\}$. In this case, Eq. (11) is not sufficient. Let us define $\{\alpha_r\}$ as

$$\{\alpha_r\} = \alpha_0\{1\} + \{\alpha_g\} \tag{12}$$

Equation (12) indicates that at zero airspeed each wing panel has a common angle of attack α_0, plus an additional known set of angles of attack $\{\alpha_g\}$, due to known gravitational (in-

ertial) loads. The parameter α_0 is determined by equating the total wing lift to the aircraft gross weight W. This equation is written as

$$\{h_j\}^T\{p_j\} = W \tag{13}$$

The magnitude of $\{\alpha_g\}$ is computed from a load-flexibility relationship, similar to Eq. (3), with $\{p_j\}$ replaced by the weights of each panel acting at the panel centers of gravity. This relationship has the following form:

$$\{\alpha_g\} = [D_{ij}]\{w_j\} \tag{14}$$

where w_j is the weight of each wing panel. This relationship also can be written in terms of aircraft gross weight as follows:

$$\{\alpha_g\} = [D_{ij}]\{\bar{w}_i\}fW \tag{15}$$

The parameter f is the ratio of total wing weight to aircraft gross weight. As a result, $\bar{w}_i$ is a nondimensional wing panel weight.

For this study, pitch trim was not considered. When Eqs. (11–13) and (15) are combined, they define a relationship among W, α_0, and δ_0. After some algebraic manipulation, this relationship takes on the following form:

$$\begin{bmatrix} A_1 & A_2 \\ B_1 & B_2 \end{bmatrix} \begin{Bmatrix} \delta_0 \\ \alpha_0 \end{Bmatrix} = \frac{WL^2}{EI} \begin{Bmatrix} 1 - fA_3 \\ -B_3 f \end{Bmatrix} \tag{16}$$

The coefficients A_i and B_i are nondimensional functions of sweep angle Λ, dynamic pressure, structural flexibility, and planform geometric parameters. The parameter EI is a reference wing bending stiffness, while L is the wingspan dimension, measured along the swept span and independent of sweep angle.

Solving for δ_0 and α_0, in terms of the parameters in Eq. (16) we find

$$\delta_0 = \frac{WL^2}{EI}\left[\frac{B_2 + f(A_2B_3 - A_3B_2)}{A_1B_2 - A_2B_1}\right] \tag{17}$$

$$\alpha_0 = \frac{WL^2}{EI}\left[\frac{-B_1 + f(B_1A_3 - A_1B_3)}{A_1B_2 - B_1A_2}\right] \tag{18}$$

These equations can be written more simply in nondimensional form as

$$\delta_0 = \frac{WL^2}{EI}(b_1 + fb_2) \tag{19}$$

$$\alpha_0 = \frac{WL^2}{EI}(a_1 + fa_2) \tag{20}$$

The terms in the numerator in Eq. (11) explain the source of the need for control surface deflection δ_0. If the wing were geometrically and structurally symmetrical, this numerator would be zero. The denominator in Eq. (11) is defined as the aileron "rolling power" (the aileron roll moment generated per unit δ_0). This denominator is amplified (or attenuated) by aeroelastic effects represented by multiplication by $[B_{ij}]^{-1}$. The first term inside the second set of brackets, proportional to $\partial\alpha/\partial\delta$, is unaffected by dynamic pressure; while the second term, containing the term $qc_{m\delta}[E_{ij}]$, depends upon wing flexibility, dynamic pressure, and $c_{m\delta}$. The term $\partial\alpha/\partial\delta$ is greater than zero; the second term (because $c_{m\delta}$ is negative), becomes a progressively larger negative number as q increases. Because of this, the aileron rolling power will become zero at a value of q called the reversal dynamic pressure, and denoted as q_R. Near this dynamic pressure Eq. (11) appears to predict large aileron deflections. However, since changes in laminate stiffness will affect both the numerator and denominator, one must be careful to consider the ratio in Eq. (11), not just individual terms.

Roll Trim Tailoring of a High Aspect Ratio Untapered Oblique Wing

To illustrate the potential effects on oblique wing roll trim requirements, as the result of introducing wing laminate stiffness cross coupling into an oblique wing design, a simple planform was chosen. It was patterned after a series of wind-tunnel models, constructed of flat aluminum sheets, that were used for low-speed oblique wing testing at Virginia Polytechnic Institute and State University in the mid-1970s.[16] These wind-tunnel models provided a means to correlate theory and experiments involving metallic oblique wing static and dynamic aeroelastic behavior. Similar laminated composite wings were also tested to examine forward swept wing aeroelasticity.[17]

The laminate and wing planform geometry are shown in Fig. 5. Table 1 provides the wing baseline structural and aerodynamic parameters. A computer code, CWINGC, with oblique wing static aeroelastic analysis capability[18] based on the procedure outlined previously, was used to perform the computations.

A spanwise asymmetrical laminate is used on the fore and aft swept wing portions and is created by a continuous set of plies (Fig. 5). For this study, the bending and torsional stiffness, EI and GJ, were held fixed while stiffness crosscoupling Ψ was treated as an independent parameter. The bend/twist parameter is determined from the following relationship:

$$K = \Psi\sqrt{EI \cdot GJ} \tag{21}$$

When laminate plies on the forward wing portion are rotated forward, an elastic washout effect is produced in which upward bending is accompanied by nose-down twist as shown in Fig. 3b. In this case, Ψ (and K) are negative. Plies swept aft, on the aft swept wing portion of Fig. 5, produce a wash-in effect that amplifies the lift; both K and Ψ are positive for this portion.

CWINGC calculations predict that when $\Psi = 0$, this clamped 30-deg oblique wing will diverge at an airspeed of 107.77 ft/s

Table 1 Baseline geometrical and stiffness parameters for an orthotropic oblique wing configuration

L = 17.32 in.	GJ = 1398.0 lb-in.^{2}	
c = 4.619 in.	EI = 917.5 lb-in.^{2}	m = 0.02956 lb/in.
$\frac{\partial\alpha}{\partial\delta}$ = 0.4	$c_{m\delta}$ = −0.500	Λ = 30 deg

Aileron surfaces located between 0.6 and 0.9L.

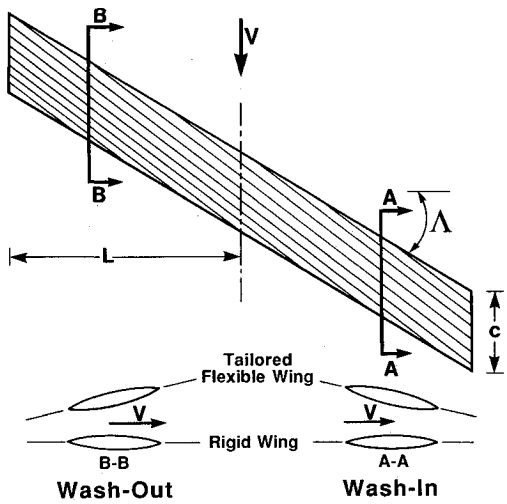

Fig. 5 30-deg oblique wing with asymmetrical ply orientation.

at sea level. This divergence speed is slightly larger than that computed for a similar symmetrical forward swept wing. Figure 6 shows that the oblique wing divergence velocity increases rapidly as the bend/twist stiffness cross coupling parameter Ψ is increased from zero. However, near $\Psi = 0.7$, there is a cusp in the stability boundary, indicative of an instability mode switching phenomenon. At this point, divergence speed decreases, and further increases in Ψ are counterproductive.

If only the forward swept wing portion were present, further increases in Ψ beyond 0.7 would increase its divergence speed. However, because of the ply arrangement chosen, when washout is increased on the forward swept wing, wash-in is increased on the aft swept wing. This increased wash-in decreases the divergence speed of an "isolated" aft swept wing. Near $\Psi = 0.7$, the divergence speeds of the isolated fore and aft wing portions are identical. For values above $\Psi = 0.7$, the aeroelastic behavior of aft swept wing "drives" the process and produces the critical divergence mode.

Studies of symmetrical swept wing divergence have developed closed-form expressions for the divergence dynamic pressures of idealized symmetrical lifting surfaces. Because of well-known limitations due to aerodynamic strip theory, use of these idealizations is more restricted than are those for the present model. One such algebraic formula[15] is written as follows:

$$q_D = \left[\frac{2.47(1 - \Psi^2)}{cL^3 c_{l_\alpha} \cos^2\Lambda}\right] \times \left\{\frac{GJ(L/e)}{1 - \Psi\sqrt{R}\tan\Lambda - 0.39(R)(L/e)[\tan\Lambda - (\Psi/\sqrt{R})]}\right\} \quad (22)$$

Certain ranges of values of Ψ may cause the denominator of Eq. (22) to be negative; when q_D is negative, divergence cannot occur because the resulting airspeed is imaginary. (Note that, in Eq. (22), L, e, and c are the swept wing spanwise dimensions for semispan, distance between the aerodynamic center and reference axis, and chord, respectively.)

With the exception of Λ and Ψ, the parameters appearing in Eq. (22) are identical for both the fore and aft swept wing portions. At the cusp point shown in Fig. 6, the divergence airspeeds of the isolated swept forward and swept back wings should be nearly identical. Equation (22) predicts that fore/aft wing divergence speeds will be identical when the following relationship is satisfied:

$$\tan\Lambda = \Psi/\sqrt{R} \quad (23)$$

Here Λ is the oblique wing sweep angle shown in Fig. 5 and (always positive), while Ψ is the magnitude of the oblique wing cross coupling (positive on the sweptback wing and negative on the sweptforward portion). For $R = 1.52$, Eq. (23) predicts divergence equality of the 30-deg forward swept/aft swept divergence dynamic pressures when $\Psi = 0.7127$. This prediction correlates extremely well with the location of the cusp for the data shown in Fig. 6.

This analysis was repeated, using both CWINGC and Eq. (23), with $R = 0.5$ (EI in Table 1 was increased, while GJ remained constant). In this case, Eq. (23) predicts wing divergence equality to occur when $\Psi = 0.4082$. The accuracy of this result is confirmed by inspection of Fig. 6.

One can view Eq. (23) as defining the condition under which a measure of spanwise static aeroelastic "symmetry" between fore and aft wing exists. Since Ψ is bounded [see Eq. (4)], there is a theoretical maximum oblique wing sweep angle for which aeroelastic tailoring is effective in generating this symmetry. If this angle is denoted as Λ_m and we set Ψ equal to its maximum value—unity—then Eq. (23) provides the following value for Λ_m:

$$\Lambda_m = \tan^{-1}\sqrt{(EI/GJ)} = \tan^{-1}\sqrt{(1/R)} \quad (24)$$

When $R = 1.52$, then $\Lambda_m = 39.01$ deg, while for $R = 0.5$ we find that $\Lambda_m = 54.74$ deg. Equation (24) indicates that for fixed values of GJ, larger values of EI are desirable. Note also that when EI is large, oblique wing aeroelastic effects become less important, and when Ψ is near unity, the wing is very flexible.

Tailoring to Reduce the Need for Roll Trim

The effect of introducing bend/twist deformation coupling to reduce the need for aileron roll control will be examined by considering two cases. The first has no cross coupling. The values of b_1 and b_2 [Eq. (19)] for this 30-deg oblique wing were computed at several airspeeds when $\Psi = 0$. Plots of these two parameters, vs nondimensional velocity, are shown in Fig. 7. (Note that $-b_2$ rather than b_2 is plotted in Fig. 7.) The reference airspeed for nondimensionalization is $V_D = 107.77$ ft/s, the clamped oblique wing divergence airspeed when $\Psi = 0$.

When the nondimensional airspeed is low (the situation depicted in Fig. 2 when the wing is "rigid"), roll trim requires that lift be added to the swept forward wing portion by deflecting its aileron downward. On the aft wing the aileron is deflected upward ($\delta_0 < 0$) to create a roll-trimmed wing. The term b_1 is proportional to the ratio of unbalanced roll moment of the wing, due to α_0, divided by the aileron rolling power (moment). Figure 7 shows that the term b_1 is a large negative number when V is a small fraction of V_D. This large number is the result of roll unbalance due to "rigid wing" aerodynamic

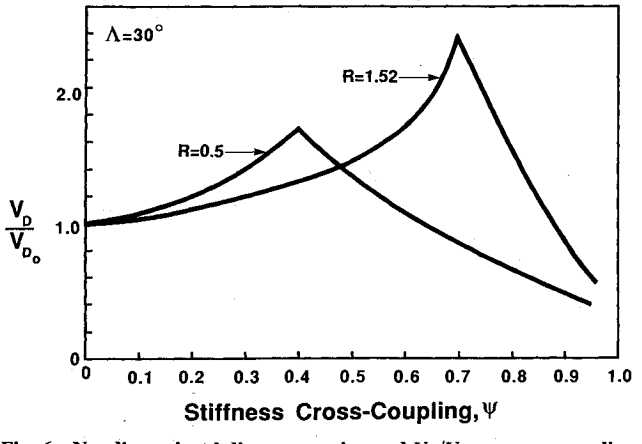

Fig. 6 Nondimensional divergence airspeed V_D/V_{D0} vs cross coupling parameter Ψ for 30-deg oblique wing showing results for two values of $R = GJ/EI$.

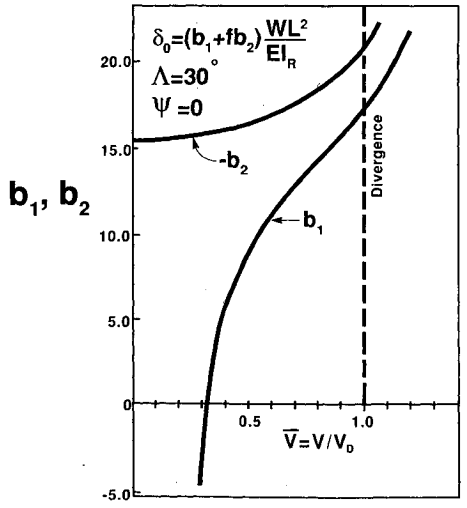

Fig. 7 Coefficients b_1 and b_2 [Eq. (19)] vs airspeed parameter $\bar{V} = V/V_D$; 30-deg orthotropic oblique wing ($\Psi = 0$).

effects, and because the expression for δ_0 in Eq. (19) is arbitrarily divided by the bending stiffness EI.

In Fig. 7, as the nondimensional airspeed $\bar{V} = V/V_D$ increases, aeroelastic deformation becomes more important and b_1 declines. At $\bar{V} = 0.31$, the unbalanced roll moment due to aeroelastic flexibility exactly cancels the unbalanced roll moment of the rigid wing, and b_1 is zero in Fig. 7. As airspeed increases further, the unbalanced aeroelastic roll moment increases and b_1 increases.

The term b_2 appears because the weight of the flexible wing causes it to bend downward, creating a distributed streamwise angle of attack at zero airspeed. The result is a built-in gravity, or inertia-induced, angle of attack. Note that b_2 is always negative, meaning that at high speeds the gravity-induced angle of attack actually provides a beneficial roll moment to trim the aircraft. As a result, for reasonable values of f (the ratio of total wing weight to total aircraft weight) i.e., 0.1–0.2), the relationship between δ_0 and $\bar{V}$ will resemble closely the b_1 vs $\bar{V}$ relationship, but displaced slightly to the right in Fig. 7.

Notice that at $\bar{V} = 1$ (the divergence airspeed) $[B_{ij}]$ is singular, although no discontinuities are apparent in the curves shown in Fig. 7. Notice that Eq. (16) defines a static feedback control relationship that couples together δ_0, α_0, and W. Both the determinant of $[B_{ij}]$ and the term $A_1B_2 - A_2B_1$ enter into the computation of a_i and b_i. The coefficients A_i and B_i can be written as $\hat{A}_i/\Delta$ and $\hat{B}_i/\Delta$ (where Δ is the determinant of $[B_{ij}]$. Then a_1, a_2, b_1, and b_2 appear in the following form:

$$a_1 = \frac{-\hat{B}_1\Delta}{\hat{A}_1\hat{B}_2 - \hat{A}_2\hat{B}_1} \tag{25}$$

$$a_2 = \frac{\hat{A}_3\hat{B}_1 - \hat{A}_1\hat{B}_3}{\hat{A}_1\hat{B}_2 - \hat{A}_2\hat{B}_1} \tag{26}$$

$$b_1 = \frac{\hat{B}_2\Delta}{(\hat{A}_1\hat{B}_2 - \hat{A}_2\hat{B}_1)} \tag{27}$$

$$b_2 = \frac{(\hat{A}_2\hat{B}_3 - \hat{A}_3\hat{B}_2)}{\hat{A}_1\hat{B}_2 - \hat{A}_2\hat{B}_1} \tag{28}$$

Equations (26) and (28) indicate that a_2 and b_2 do not depend on the value of the determinant Δ. However, the terms a_1 and b_1 are proportional to the determinant of $[B_{ij}]$. As a result, we might expect a_1 and b_1 to be zero at $\bar{V} = 1$. However, Fig. 7 (as well as extensive computational checks using CWINGC) shows that this is not so.

When the value of the determinant $\hat{\Delta} = \hat{A}_1\hat{B}_2 - \hat{A}_2\hat{B}_1$ is computed as a function of $\bar{V}$, it is found to be zero when $\bar{V} = 1$. This leads to a situation where, because of cancelling singularities ($\Delta/\hat{\Delta}$), the values of b_1 and a_1 are nonzero at $\bar{V} = 1$. The terms $\hat{A}_2\hat{B}_3 - \hat{A}_3\hat{B}_2$ and $\hat{A}_3\hat{B}_1 - \hat{A}_1\hat{B}_3$ were also computed as functions of $\bar{V}$, and also found to be zero at $\bar{V} = 1$. As a result, finite, nonzero values of a_2 and b_2 appear at $\bar{V} = 1$.

These latter results appear to indicate that statically coupling the differential aileron displacement together with aeroelastic deformation produces a static aeroelastic instability at a value of q identical to the divergence q of the clamped wing. This indicates that, although the classical clamped wing divergence instability is not present, roll trim at this flight condition may be difficult. These results deserve a more detailed examination, but were not considered in this study.

Returning to our original discussion, we can attempt to create "aeroelastic symmetry" to reduce the need for roll trim. Figure 6 shows that this occurs when Ψ has a value near 0.71. Figure 8 shows the altered behavior of b_1 and b_2, as functions of $\bar{V}$, for a configuration with Ψ chosen to be a slightly lesser value, $\Psi = 0.695$. This value was chosen to place the aileron reversal speed at an airspeed slightly less than the divergence speed ($\bar{V}_R = 0.95$). For this value of Ψ, the divergence speed

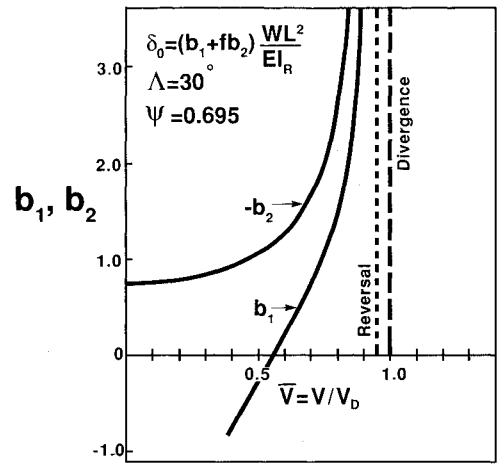

Fig. 8 Coefficients b_1 and b_2 [Eq. (19)] vs airspeed parameter $\bar{V} = V/V_D$; 30-deg oblique wing with (asymmetrical) $\Psi = 0.695$.

is over two times that of the wing with no cross coupling ($\Psi = 0$).

Comparing Figs. 7 and 8, note that when $\Psi = 0.695$, the point when $b_1 = 0$ occurs at a larger nondimensional airspeed when compared to the wing with $\Psi = 0$. The values of b_1 and b_2 in Fig. 8 are about one-tenth those in Fig. 7, reflecting the effectiveness of aeroelastic tailoring in reducing the need for aileron roll trim. On the other hand, the values of b_1 and b_2 shown in Fig. 8 increase rapidly near $\bar{V} = 0.95$. Near this airspeed, aircraft roll trim requires large values of δ_0, even though the actual oblique wing roll moment to be controlled is smaller than before. This occurs because laminate tailoring to create aeroelastic symmetry and reduce the roll moment has reordered the relative positions of the reversal airspeed and the divergence airspeed. The presence of a conflict or tradeoff between divergence and aileron reversal indicates that an integrated design approach that considers the effect of aircraft aeroelastic flexibility on both control effectiveness and passive roll trim should be used. It is to this consideration that we now turn our attention.

Tailoring to Position the Control Reversal Airspeed with Respect to Divergence

The effects on the control reversal airspeed of introducing bend/twist stiffness cross coupling are examined more closely. Define the denominator of Eq. (11) as M_R (the aileron rolling power) and write it in the following form:

$$M_R = \left(qM_{m\delta}c_{m\delta} + M_{m\alpha}\frac{\partial\alpha}{\partial\delta}\right)\delta_0 \tag{29}$$

At aileron reversal, q is equal to q_R, and M_R is zero. Equation (29) then reduces to the following relationship:

$$c_{m\delta}\left[\frac{\partial\alpha}{\partial\delta}\right]^{-1} = c_{m\delta}\frac{c_{l_\alpha}}{c_{l_\delta}} = \left.\frac{-M_{m\alpha}}{q_RM_{m\delta}}\right|_{q=q_R} \tag{30}$$

Note that both $M_{m\alpha}$ and $M_{m\delta}$ are functions of q and structural flexibility parameters.

Although Eq. (30) does not provide an expression for q_R in closed form (since dynamic pressure q also appears in the coefficients $M_{m\alpha}$ and $M_{m\delta}$), it shows the interrelationship between the aerodynamic derivatives and the wing aeroelastic parameters. The derivatives $c_{m\delta}$ and $\partial\alpha/\partial\delta$ are functions of aileron flap-to-chord ratio.[10] Equation (30) indicates that the value of q_R can be adjusted by tailoring the values of $c_{m\delta}$ and $\partial\alpha/\partial\delta$. Such an adjustment might have the objective of maximizing the aileron reversal speed with respect to a structural parameter (such as Ψ), and with respect to a control system parameter such as aileron flap-to-chord ratio.

The three aerodynamic coefficients $c_{m\delta}$, $c_{l\alpha}$, and $c_{l\delta}$ are Mach number and sweep angle dependent, as are the expressions for $M_{m\alpha}$ and $M_{m\delta}$. To determine q_R in a simple manner, we could plot the left and right sides of Eq. (30) against Mach number at a specific altitude and find a common crossing point; this crossing is the reversal Mach number. When multiplied by the local speed of sound, the reversal Mach number determines the aileron reversal speed V_R. There is a simpler way to do this.

For the example being considered, dynamic pressure and aerodynamic derivatives $c_{l\delta}$, $c_{m\delta}$, $c_{l\delta}$ always appear as products qc_{l_δ}, qc_{l_α}, qc_{m_δ}. We can write these products as

$$qc_{l_\delta} = q'c^0_{l\delta} \tag{31a}$$

$$qc_{l_\alpha} = q'c^0_{l\alpha} \tag{31b}$$

$$qc_{m_\delta} = q'c^0_{m\delta} \tag{31c}$$

where q' is a dynamic pressure parameter defined as

$$q' = [q/(1 - M^2\cos^2\Lambda)^{1/2}] \tag{32}$$

The denominator in Eq. (32) provides the standard correction of two-dimensional aerodynamic coefficients for Mach number and sweep. The notation $(\,)^0$ refers to the value of an incompressible sectional aerodynamic coefficient. Equation (30) then can be written as

$$c^0_{m\delta}\left[\frac{\partial\alpha^0}{\partial\delta}\right]^{-1} = \left.\frac{-M_{m\alpha}}{q'_R M_{m\delta}}\right|_{q'=q'_R} \tag{33}$$

With sweep angle fixed at 30 deg, the ratio on the right side of Eq. (33) can be plotted vs $q' \cdot c^0_{m\delta}(c^0_{l_\alpha}/c^0_{l\delta})$. Reversal will occur when the term on the left side of Eq. (33) equals this dynamic pressure parameter.

A procedure for determining the reversal speed can be developed by defining a new parameter k as follows:

$$k = (M_{m\alpha}/q'M_{m\delta})q' = (M_{m\alpha}/M_{m\delta}) \tag{34}$$

This term still depends implicitly on the pressure parameter. At reversal, the relationship between wing and control surface aerodynamic derivatives and aeroelastic parameters then becomes

$$c^0_{m\delta}(c^0_{l_\alpha}/c^0_{l\delta}) = (-k_R/q'_R) \tag{35}$$

where k_R is the value of Eq. (34) calculated at reversal. The reversal dynamic pressure parameter is then found from

$$q'_R = (-k_R/c^0_{m\delta})(c^0_{l\delta}/c^0_{l_\alpha}) \tag{36}$$

From the examination of numerous CWINGSM computations, k values computed when q' is well below q'_R, are found to be only slightly different than k_R. As a result, subcritical values of k can be used in place of k_R in Eq. (36) to provide an excellent estimator for q'_R. This procedure appears similar to that discussed in Ref. 14 and attributed to Lawrence and Sears.[19]

This procedure was used to compute values of q'_R as a function of Ψ, using data for the example wing shown in Table 1. Figure 9 plots these values of q'_R normalized with respect to q'_{R_0}, the value of q'_R when $\Psi = 0$. Also shown in Fig. 9 is the divergence dynamic pressure parameter q'_D, similarly nondimensionalized, plotted as a function of Ψ. Note that the maximum value of q'_R (and k_R) occurs near $\Psi = 0.71$, the value at which the fore/aft divergence speeds are identical. The Mach numbers at which reversal and divergence occur at a given value of Ψ are so small ($M < 0.2$) that q' and q are essentially identical.

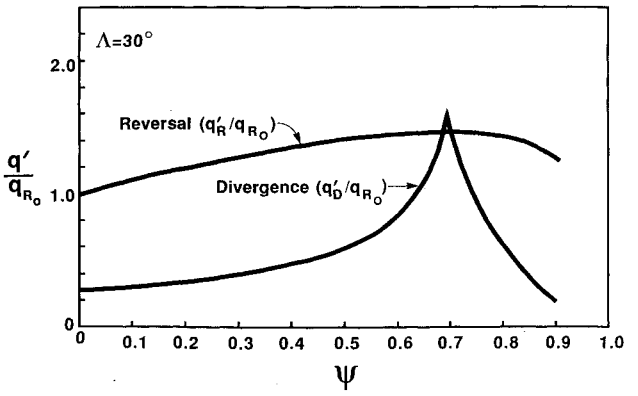

Fig. 9 Nondimensional aileron reversal parameter q'_R/q_{R0} and divergence parameter q'_D/q_{R0} vs Ψ. Parameters are nondimensionalized with respect to q_{R0}, the reversal dynamic pressure with $\Psi = 0$.

The two curves defining divergence and reversal intersect near $\Psi = 0.68$. Oblique wing configurations with asymmetrical bend/twist stiffness cross coupling values below $\Psi = 0.68$ have a clamped divergence speed below aileron reversal. For a range of values between $\Psi = 0.68$ and $\Psi = 0.73$, the reversal speed is less than the divergence speed. A more favorable situation would occur if q_R and q_D were identical, but this cannot be so unless the control surfaces are resized [to change the left side of Eq. (35)] or repositioned [to change the right side of Eq. (35)].

The q'_R vs Ψ curve can be repositioned with respect to the q'_D curve by changing either the spanwise location or size of the ailerons. The result would be an oblique wing with both aileron effectiveness and divergence speed maximized, and presumably with aeroelastic roll minimized. The maximum value of q_R would coincide with the divergence cusp point. Such a resizing presents itself as an optimization problem with a control surface performance index used together with structural design variables.

Conclusions

Although there currently is no major effort directed towards the development of an oblique wing aircraft, the concept continues to have technical merit and appeal. As with all design concepts, there are a myriad of conflicting design objectives that must be reconciled to produce a feasible aircraft. Some of these objectives require aeroelastic considerations of the type discussed in this article. It remains to be seen whether the aeroelastic roll unbalance phenomenon detailed in this study is a significant problem in the design of a real oblique wing aircraft, capable of operating at supersonic speeds, whose structure, unlike that considered in the present study, is constrained to conform to many different requirements. However, the elementary planform used in this study suggests that the problem is intrinsic to an efficient, and therefore, flexible, oblique wing structure.

Should the aeroelastic roll trim problem be significant, this study has shown that bend/twist deformation coupling of the type introduced by laminate orientation can lead to a substantial reduction in the magnitude of this problem. The present study also shows that by reducing the need for roll trim, one may introduce an aileron effectiveness problem that was not previously present. The introduction of such a difficulty is particularly annoying since the structural tailoring solution to roll trim is a "point design" solution requiring the addition of aileron control in "off-design" speed regimes.

The interaction between the amount of aeroelastic tailoring necessary to relieve one aeroelastic difficulty, while still retaining enough authority over a related aeroelastically driven area, is a classical optimization problem. The significant feature of this problem, as implied by the oblique wing study presented in this article, is that a creative solution requires the cooperation between the group whose responsibility it is

to design the control surfaces (and their placement) and the structural design group. This type of problem falls under the heading of a controls/structure interaction effort sometimes simply referred to as CSI. The formal statement of this problem and its solution requires an interdisciplinary optimization effort of a kind not yet encountered with great frequency, but of the type likely to occur more often as demands for efficiency and technological cross fertilization or "hybridization" continue. The discussion related to aileron reversal, and the interplay between it and wing divergence, showed the potential benefits of such an exercise, without claiming to present a state-of-the-art method for accomplishing this objective.

Finally, as a related issue, the subject of instability of a controlled, roll trimmed oblique wing was identified as one that deserves further investigation. Singularities of the type that usually signal the presence of a static instability were uncovered during the computational phase of the study. Since the calculations discussed in this article deal primarily with equilibrium, not stability, these singularities were not investigated in detail, but are an interesting and perhaps important subject of future work, should the oblique wing concept gain serious attention.

Acknowledgments

This research was sponsored by the Naval Air Development Center, under Contract N62269-85-C-0268. Robert Richey was the Technical Monitor. The author also wishes to acknowledge the excellent, cogent reviews of this manuscript that suggested the inclusion of the discussion for Eqs. (25–28).

References

[1]Jones, R. T., "New Design Goals and a New Shape for the SST," *Astronautics and Aeronautics*, Vol. 10, Dec. 1972, pp. 66–70.

[2]Gregory, T. A., "Oblique Wing Ready for Research Aircraft," *Aerospace America*, Vol. 23, No. 6, 1985, pp. 78–83.

[3]Weisshaar, T. A., "Influence of Static Aeroelasticity on Oblique Wing Aircraft," *Journal of Aircraft*, Vol. 11, No. 4, 1974, pp. 247–249.

[4]Weisshaar, T. A., and Crittenden, J. B., "Flutter of Asymmetrically Swept Wings," *AIAA Journal*, Vol. 14, No. 8, 1976, pp. 993, 994.

[5]Jones, R. T., and Nisbet, J. W., "Aeroelastic Stability and Control of an Oblique Wing," *The Journal of the Royal Aeronautical Society*, Vol. 80, Aug. 1976, pp. 365–369.

[6]Crittenden, J. B., Weisshaar, T. A., Johnson, E. H., and Rutkowski, M. J., "Aeroelastic Stability Characteristics of an Oblique-Wing Aircraft," *Journal of Aircraft*, Vol. 15, No. 7, 1978, pp. 429–434.

[7]Weisshaar, T. A., "Lateral Equilibrium of Asymmetrical Swept Wings: Aileron Control vs Geometric Twist," *Journal of Aircraft*, Vol. 14, No. 2, 1977, pp. 122–127.

[8]Shirk, M. H., Hertz, T. J., and Weisshaar, T. A., "Aeroelastic Tailoring—Theory, Practice, Promise," *Journal of Aircraft*, Vol. 23, No. 1, 1986, pp. 6–18.

[9]Weisshaar, T. A., "Aeroelastic Tailoring—Creative Uses of Unusual Materials," AIAA/ASME/ASCE/AHS/ASC 28th Structures, Structural Dynamics and Materials Conf., AIAA Paper 87-0976, Monterey, CA, April 1987.

[10]Fung, Y. C., *An Introduction to the Theory of Aeroelasticity*, Dover, New York, 1969, pp. 113–119.

[11]Sensburg, O., and Schmidinger, G., "Integrated Design of Structures," Flight Symposium: Improvement of Combat Performance for Existing and Future Aircraft, AGARD, Treviso, Italy, April 1986.

[12]Weisshaar, T. A., and Nam, C., "Aeroservoelastic Tailoring for Lateral Control Enhancement," *Recent Advances in Multidisciplinary Analysis and Optimization: NASA Conference Publication 3031*, Hampton, VA, Sept. 1989, pp. 803–814.

[13]Gray, W. L., and Schenk, K. L., "A Method for Calculating the Subsonic Steady-State Loading on an Airplane with a Wing of Arbitrary Planform and Stiffness," NACA TN 3030, July 1953.

[14]Bisplinghoff, R. L., Ashley, H., and Halfman, R. L., *Aeroelasticity*, Addison-Wesley, Reading, MA, 1955, pp. 462–469, 506–510.

[15]Weisshaar, T. A., "Forward Swept Wing Aeroelasticity," Air Force Flight Dynamics Lab., TR-79-3087, Wright-Patterson AFB, OH, June 1979.

[16]Papadales, B. S., "An Experimental Investigation of Oblique Wing Static Aeroelastic Phenomena," M.S. Thesis, Dept. of Aerospace and Ocean Engineering, Virginia Polytechnic Inst. and State Univ., Blacksburg, VA, 1975.

[17]Blair, M., and Weisshaar, T. A., "Swept Composite Wing Aeroelastic Divergence Experiments," *Journal of Aircraft*, Vol. 19, No. 11, 1982, pp. 1019–1024.

[18]Weisshaar, T. A., "CWINGC-Composite Static Aeroelastic Analysis of Oblique Wings-User's Guide," School of Aeronautics and Astronautics, Purdue Univ., West Lafayette, IN, Aug. 1985.

[19]Lawrence, H. R., and Sears, W. R., "Three-Dimensional Wing Theory for the Elastic Wing," Northrop Aircraft, Rept. A-59, Los Angeles, CA, June 1944.